



*Citation for published version:*

Hu, Y, Liang, W, Xie, M, Chen, G, Yoong Loh, C, Huang, M & Qiao, J 2023, 'Optimization of a continuous flow electrocoagulation as pretreatment for membrane distillation of the waste stream in vinyl ester resin production', *Separation and Purification Technology*, vol. 318, 124004. <https://doi.org/10.1016/j.seppur.2023.124004>

*DOI:*

[10.1016/j.seppur.2023.124004](https://doi.org/10.1016/j.seppur.2023.124004)

*Publication date:*

2023

*Document Version*

Peer reviewed version

[Link to publication](#)

*Publisher Rights*

CC BY-NC-ND

**University of Bath**

**Alternative formats**

If you require this document in an alternative format, please contact:  
[openaccess@bath.ac.uk](mailto:openaccess@bath.ac.uk)

**General rights**

Copyright and moral rights for the publications made accessible in the public portal are retained by the authors and/or other copyright owners and it is a condition of accessing publications that users recognise and abide by the legal requirements associated with these rights.

**Take down policy**

If you believe that this document breaches copyright please contact us providing details, and we will remove access to the work immediately and investigate your claim.

1 **Optimization of a continuous flow electrocoagulation as**  
2 **pretreatment for membrane distillation of the waste stream**  
3 **in vinyl ester resin production**

4

5 Yuan Hu<sup>1</sup>, Weihan Liang<sup>1</sup>, Ming Xie<sup>2</sup>, Gang Chen<sup>1\*</sup>, Ching Yoong Loh<sup>2</sup>, Manhong

6 Huang<sup>1</sup>, Jinli Qiao<sup>1</sup>

7

8 <sup>1</sup>Textile Pollution Controlling Engineering Centre of Ministry of Environmental

9 Protection, College of Environmental Science and Engineering, Donghua University,

10 Shanghai 201620, China

11 <sup>2</sup>Department of Chemical Engineering, University of Bath, BA2 7AY, UK

12

13

14

15

16

17 Email: cheng@dhu.edu.cn (G. Chen); phone: +86-21-67792546

18 **Abstract**

19 Vinyl ester resin production wastewater (VERW) contains high concentrations of  
20 organics particularly, methacrylic acid and bisphenol A, which are hazardous chemicals  
21 and harmful to the aquatic environment. Therefore, there is an urgent need to properly  
22 treat the effluent before discharge into the aquatic system. In this work, direct contact  
23 membrane distillation (DCMD) was explored as an advanced treatment of the VERW  
24 pre-treated by a continuous flow electrocoagulation (EC) and peroxi-electrocoagulation  
25 (PEC) processes. Optimization of EC and PEC processes were investigated and the  
26 DCMD performance was evaluated. Results showed that the optimal value of current  
27 density and polyacrylamide (PAM) dosage was  $15 \text{ mA/cm}^2$  and  $1 \text{ mg/L}$ , respectively in  
28 the EC process. For the PEC process, the optimal addition of hydrogen peroxide ( $\text{H}_2\text{O}_2$ )  
29 dosage was four times of the chemical oxygen demand (COD) concentration of EC  
30 effluent. The COD of VERW was effectively removed via EC followed by PEC (EC-  
31 PEC), resulting in the significant alleviation of membrane fouling during DCMD  
32 filtration of VERW. The initial flux of DCMD filtration of VERW pre-treated via EC-  
33 PEC improved by 35%, compared that only pre-treated by EC. Moreover, the  
34 concentration factor (CF) of the DCMD system reached up to 8.1 and the conductivity  
35 of distillate was less than  $33.2 \text{ }\mu\text{S/cm}$ . Hence, the EC and membrane distillation hybrid  
36 process paves a new way for the effective treatment of waste steam from resin  
37 production.

38 **Keywords:** VERW; EC; Peroxi-electrocoagulation; DCMD; Saline high organic  
39 wastewater

## 40 **1. Introduction**

41 Vinyl ester resin (VER) is a thermosetting-modified epoxy resin obtained by the  
42 reaction of bisphenol-type or phenolic-type epoxy resin with methacrylic acid<sup>[1, 2]</sup>. It is  
43 a high-quality matrix for anti-corrosion composite materials such as glass fiber-  
44 reinforced plastics<sup>[1, 3, 4]</sup>, and widely used in a wide range of industrial processes, such  
45 as automobile, petrochemical and, electronic information industry<sup>[5, 6]</sup>. However, during  
46 the VER manufacturing process, a large amount of alkaline production wastewater  
47 containing methacrylic acid and bisphenol A (BPA) is generated, which is difficult to  
48 treat because of the high salinity, high COD concentration, and low biodegradability<sup>[7,</sup>  
49 <sup>8]</sup>. Therefore, the effective treatment of this type of wastewater is urgently needed.

50 Membrane distillation (MD) has received attention because of its effectiveness in  
51 treating high-salinity wastewater. Compared to conventional pressure-driven  
52 membrane processes (e.g., nanofiltration, reverse osmosis), MD can be operated under  
53 normal pressure and allows only volatile substances to pass through porous  
54 hydrophobic membranes, with almost 100% of non-volatile substances rejection and  
55 high-quality water recovery<sup>[9-12]</sup>. In addition, the operating temperature of MD is lower  
56 than that of traditional distillation processes with the possibility of using waste heat as  
57 energy input<sup>[13, 14]</sup>. Lokare et al. showed that treating shale gas produced water with  
58 DCMD using exhaust gas from a natural gas compression station as a waste heat source  
59 was sufficient to concentrate all produced water produced in Pennsylvania to 30wt %<sup>[15]</sup>.  
60 Recently, MD technology has been widely applied in seawater desalination, high-  
61 salinity wastewater treatment, and was also regarded as an effective way to achieve

62 near-zero discharge of wastewater<sup>[10, 11]</sup>. Sarallakhniknezhad et al. used DCMD to treat  
63 hypersaline drilling mud water, producing high quality distillates with water recovery  
64 of over 60%<sup>[16]</sup>. Yan et al. used DCMD process to treat reverse osmosis brine, and the  
65 water recovery rate was higher than 70%<sup>[17]</sup>. Ngo et al. used MD to purify reverse  
66 osmosis-concentrated wastewater and achieved 98% overall water recovery for potable  
67 water reuse<sup>[18]</sup>. Therefore, MD has become a promising application in the treatment of  
68 VERW to recover high quality water. However, the high concentration of refractory  
69 organics in VERW limits the application of MD<sup>[19]</sup>. First, the higher temperature at the  
70 feed side made the volatile organics pass through the membrane and destroyed the  
71 distillate quality<sup>[20]</sup>; second, once organics were adsorbed on the membrane surface,  
72 membrane fouling was accelerated, resulting in a rapid decline in membrane flux<sup>[21, 22]</sup>.  
73 Consequently, it is necessary to remove organics from VERW prior to the application  
74 of MD.

75 A variety of methods have been used to treat refractory organic wastewater with  
76 high concentration of COD, including condensation, adsorption, extraction, micro-  
77 electrolysis, Fenton oxidation, catalytic ozonation, coagulation, and sedimentation<sup>[23-</sup>  
78 <sup>28]</sup>. Coagulation is an established method to remove non-biodegradable organics<sup>[29, 30]</sup>.  
79 Particularly, compared with aluminum salt, ferric salt has better elimination effect on  
80 organic compounds<sup>[31]</sup>. Moreover, in-situ formation of ferric ions is more conducive to  
81 the coagulation of organic compounds than the direct addition of iron salts<sup>[31, 32]</sup>.  
82 Therefore, the EC process based on the in-situ formation of coagulants is expected to  
83 be an alternative treatment for the partial or total removal of organics from wastewater

84 to alleviate membrane fouling during MD process<sup>[8, 33, 34]</sup>.

85 EC is an attractive approach with the advantages of environmental compatibility,  
86 selectivity, compatible of automation, and cost-effectiveness for treating various  
87 wastewater<sup>[8]</sup>. The method includes three successive stages: (a) sacrificial anode  
88 forming coagulant; (b) demulsification and destabilization of pollutants; (c) coagulant  
89 captures pollutants to form flocs<sup>[35, 36]</sup>. Moreover, sequential batch and continuous flow  
90 are the two common modes of EC process. During the EC process, the electrolytic  
91 dissolution of metal anodes produces a variety of hydroxyl metal ion complexes, which  
92 are hydrolyzed products and readily polymerized. The monomer and polyhydroxy  
93 complexes act as adsorbents to promote the adsorption and coprecipitation of  
94 compounds<sup>[36]</sup>. The electrostatic attraction between the particles causes the destabilized  
95 pollutants to aggregate and form readily settleable flocs<sup>[37, 38]</sup>. Ikhlaiq et al. treated  
96 veterinary drug wastewater with an ozonic-catalyzed oxidation-coupled EC process.  
97 The removal efficiency of COD was 85.1% under optimal conditions<sup>[39]</sup>. Eryuruk et al.  
98 used an EC process with an iron electrode to treat poultry slaughter wastewater, and the  
99 COD removal efficiency was up to 95.5%, and the concentration decreased from 8800  
100 to 425 mg/L<sup>[36]</sup>. Al-Qodah et al. reported coupling EC process with biological treatment  
101 for industrial wastewater treatment and found EC had high efficiency on the removal  
102 of color and residual COD in water<sup>[40]</sup>. Moreover, the removal of heavy metal ions and  
103 toxic substances in wastewater by EC improved the biodegradability for biological  
104 treatment. Meanwhile, the current in the EC process stimulated microorganisms to  
105 enhance the wastewater treatment effect<sup>[41]</sup>. These favorable factors promoted the

106 development of EC process. However, some dissolved refractory organics might still  
107 be in the effluent. Some hybrid processes such as ozone-EC, PEC, adsorption-EC, and  
108 ultrasound-EC were used to further improve the removal efficiency of dissolved organic  
109 matter in EC process<sup>[34, 42]</sup>. And the PEC process is suitable to be applied in acidic  
110 condition<sup>[43]</sup>. In the PEC process, externally-added H<sub>2</sub>O<sub>2</sub> generates Fenton reactive  
111 system and synergistically works with EC<sup>[44, 45]</sup>. In this process, H<sub>2</sub>O<sub>2</sub> is used to react  
112 with ferrous ions (Fe<sup>2+</sup>) to generate hydroxyl radicals ( $\cdot$ OH) in an acidic medium, which  
113 is conducive to the degradation of organic pollutants.

114 In previous studies, the integrated EC and MD process was used as an advanced  
115 treatment approach to effectively treat various types of waste streams<sup>[46]</sup>. Chen et al.  
116 used MD combined with EC and electro-oxidation to treat concentrated landfill leachate,  
117 and the removal efficiency of the organics reached 82.2%<sup>[47]</sup>. Sardari et al. used MD  
118 combined EC to treat the produced water with high salinity, and stable water flux with  
119 negligible fouling was reported over a 434 h experimental run<sup>[14]</sup>. Jebur et al. treated  
120 hydraulic fracturing produced water with a combined process of EC, microfiltration,  
121 and MD, reducing total dissolved solids (TDS) from 245,300 to 56 mg/L, and total  
122 organic carbon (TOC) from 120 to 1 mg/L<sup>[48]</sup>. However, the existing studies on EC-  
123 coupled MD mainly focus on the improvement of MD system performance, ignoring  
124 the maximum utilization of EC pretreatment process. In addition, most EC processes  
125 investigated are sequential batch mode, and the application of continuous flow EC and  
126 PEC coupling MD process to wastewater treatment has not been reported extensively.

127 In this work, the continuous flow EC and PEC processes were used as pretreatment  
128 approaches prior to DCMD filtration of VERW. Optimization of current density,  
129 flocculant (polyacrylamide, PAM) dosage and H<sub>2</sub>O<sub>2</sub> dosage on the pretreatment  
130 performance was investigated. Mechanism of pollutant removal via the continuous flow  
131 EC and PEC processes was discussed. Additionally, system performance of DCMD  
132 filtration of VERW pre-treated by EC and PEC processes was evaluated.

133

## 134 **2. Materials and methods**

### 135 **2.1 Characteristics of VERW**

136 VERW was obtained from Shanghai Showa Polymer Co., LTD, China. The main  
137 characteristics of the VERW were summarized in Table S1. VERW was a milky solution  
138 with a conductivity of 19.3 mS/cm and an initial pH of 13.8. The VERW had high COD  
139 concentration and turbidity, up to 16,796.9 mg/L and 39,200 NTU, respectively. In  
140 addition, the concentration of NH<sub>3</sub>-N, Na<sup>+</sup>, and Ca<sup>2+</sup> was 502 mg/L, 2511.9 mg/L, and  
141 52.6 mg/L respectively.

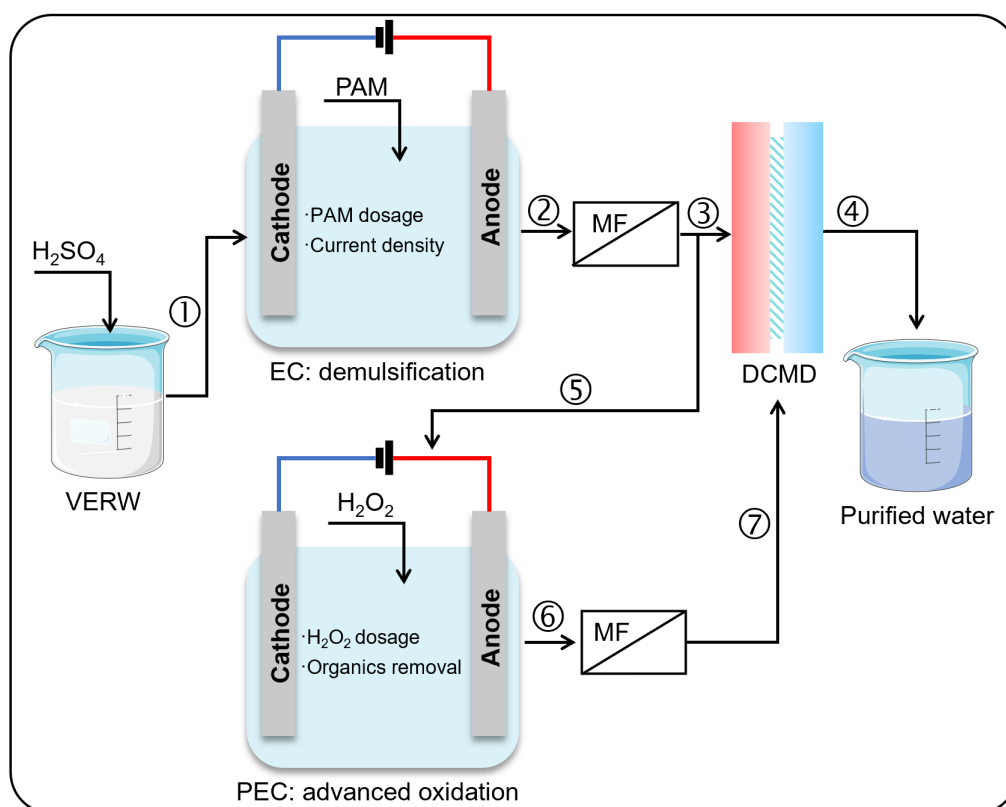
142

### 143 **2.2 Experimental setup**

144 The VERW contained large amounts of methacrylic acid and BPA with a pungent  
145 odor. The white substances in VERW cannot be removed directly through filtration with  
146 filter papers or membranes. In the actual industrial treatment process, the pollutants  
147 were removed by adding a large amount of special organic acid coagulant and bio-  
148 treatment. As shown in Table S2 and Fig.S1, single addition of flocculant, coagulant or



149 acid had no effective removal effect on pollutants. However, under acidic conditions  
 150 (pH < 1.8), the simultaneous addition of flocculant and coagulant achieved the  
 151 demulsification effect and removed pollutants. Therefore, in this work, the wastewater  
 152 was first acidified with H<sub>2</sub>SO<sub>4</sub> to a pH of 1.8. Then, pollutants were removed through  
 153 continuous flow EC&PEC (Fig.S2-3) and the voltage and quality of effluent were  
 154 recorded continuously. The stability tests showed the effluent quality was generally  
 155 stable and did not change with the volume of influent (Fig.S4)<sup>[36]</sup>. Hence, the  
 156 representative average concentrations of pollutants in samples were used to evaluate  
 157 the effluent quality. Finally, suspended particles were removed by microfiltration,  
 158 before entering the DCMD (Fig.1).



159

160 **Fig.1** Diagram of the main experimental flowchart for advanced treatment of VERW

161 pre-treated by the continuous EC and PEC processes.

162

### 163 **2.2.1 DCMD**

164 A laboratory-scale DCMD was employed in this work and a commercial flat sheet  
165 PVDF membrane (GVHP29325, nominal pore size of 0.22  $\mu\text{m}$ ) was used as the DCMD  
166 membrane (Table S3). More details of the DCMD setup can be found in our previous  
167 report<sup>[21, 46, 49]</sup>. 1200 mL of VERW and 1500 mL of deionized water were used as the  
168 feed and distillate solutions. The temperature of the feed and distillate was maintained  
169 at  $60 \pm 1^\circ\text{C}$  and  $20 \pm 1^\circ\text{C}$ . Both circulatory flow rates were 300 mL/min. After operation,  
170 the PVDF membrane was observed by field emission scanning electron microscopy  
171 with energy dispersive X-ray fluorescence spectrometer (FESEM, Hitachi SU8010,  
172 Japan) for surface morphology and scale composition identification.

173 The distillate flux ( $J$ ,  $\text{kg}/\text{m}^2\cdot\text{h}$ ) and concentration factor (CF) were calculated  
174 according to equations (9) and (10), respectively.

$$175 \quad J = \frac{\Delta W}{\Delta t \times A} \quad (1)$$

176 where  $\Delta w$  (kg) is the change of distillate mass,  $\Delta t$  (h) is the distillate collection time  
177 and  $A$  ( $\text{m}^2$ ) is the effective area of the membrane.

$$178 \quad \text{CF} = \frac{V_i}{V} \quad (2)$$

179 where  $V_i$  (L) is the initial feed volume,  $V$  (L) is the concentrated volume of the feed.

180

## 181 **2.3 Analytical methods**

### 182 **2.3.1 EC process**

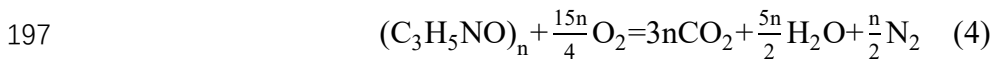
183 During the EC process, the demulsification effect would be affected by a range of

184 operating parameters, including current density, electrode connection mode, flow rate,  
 185 flocculant dosage<sup>[47, 50]</sup>. In this work, the fixed flow rate was 1000 mL/h and electrodes  
 186 were monopolar connected. The influence of current density and PAM dosage on the  
 187 EC demulsification process was investigated. The current density was calculated as  
 188 follows:

$$189 \quad CD = \frac{I}{S} \quad (3)$$

190 where CD (mA/cm<sup>2</sup>) is the current density, I (mA) is the main current, and S (cm<sup>2</sup>) is  
 191 the effective area of the electrode.

192 Floccs produced by EC treatment of resin wastewater were small and dispersed  
 193 (Fig.S1), which could be filtered and removed by adding flocculants (Table S2). PAM  
 194 as a common flocculant was used in this work. However, DCMD performance and  
 195 COD removal might be deteriorated due to the use of PAM<sup>[22, 51]</sup>. The COD contribution  
 196 of PAM (COD<sub>PAM</sub>) was calculated as follows:



$$198 \quad COD_{PAM} = \frac{4M_{PAM}}{15nM_{O_2}} C_{PAM} \quad (5)$$

199 where n is the degree of polymerization of PAM, COD<sub>PAM</sub> (mg/L) is the COD of  
 200 wastewater increased by adding PAM, M<sub>PAM</sub> (g/mol) is the molar mass of PAM, and  
 201 M<sub>O<sub>2</sub></sub> (g/mol) is the molar mass of oxygen (32 g/mol). C<sub>PAM</sub> (mg/L) is the concentration  
 202 of PAM in wastewater. Although PAM presents different molar masses due to different  
 203 degrees of polymerization, the theoretical consumption of 1 g of PAM is about 1.7 g O<sub>2</sub>,  
 204 i.e.  $\frac{4M_{PAM}}{15nM_{O_2}} \approx 1.7$ .

205 The electrical energy consumed per kilogram of COD (q) was calculated as

206 follows<sup>[52]</sup>:

$$207 \quad q = \left( \frac{I \times \int_{V_i}^{V_e} U dV}{1000 \times (V_1 - V_i)} \right) \times \left( u \times \frac{\text{COD}_i - \text{COD}_e}{10^6} \right)^{-1} \quad (6)$$

208 where  $q$  (kWh/kg COD) is the energy required for COD removal per unit mass,  $U$  (V)  
209 is trunk voltage,  $V_i$  (L) is the influent volume at the beginning of collecting EC effluent,  
210  $V_e$  (L) is the influent volume at the end of collecting EC effluent,  $u$  (L/h) is the set flow  
211 rate.  $\text{COD}_i$  (mg/L) is the initial COD concentration, and  $\text{COD}_e$  (mg/L) is the effluent  
212 COD.

213

### 214 **2.3.2 Determination of VERW composition**

215 Concentrations of metal ions in VERW were determined by inductively coupled  
216 plasma atomic emission spectrometry (Prodigy-ICP, Leeman, USA). The anion  
217 concentrations in VERW were detected with ion chromatography (Dionex Aquion IC,  
218 Thermo Fisher, USA). The concentrations of COD and ammonia nitrogen were  
219 measured by dichromate method and Nessler's reagent spectrophotometry, respectively.  
220 Turbidity was determined by turbidity meter (WGZ-1A, QIWEIYIQI, China). The  
221 removal efficiency of pollutants was calculated using the following equation:

$$222 \quad R = \frac{C_i - C_e}{C_i} \times 100\% \quad (7)$$

223 where  $R$  (%) is removal efficiency,  $C_i$  (mg/L) and  $C_e$  (mg/L) are the concentration of  
224 pollutants in influent and effluent, respectively. The composition of organics in VERW  
225 was determined by a fluorescence spectrometer (F7000, Hitachi, Japan) and subtracted  
226 the spectrum of deionized water from the EEM of all samples to correct the inner filter  
227 effects<sup>[53, 54]</sup>.

228

### 229 **3. Results and discussion**

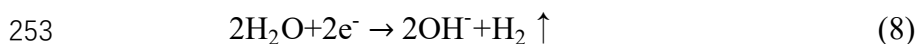
#### 230 **3.1 Demulsification of VERW via EC**

##### 231 **3.1.1 Effect of current density**

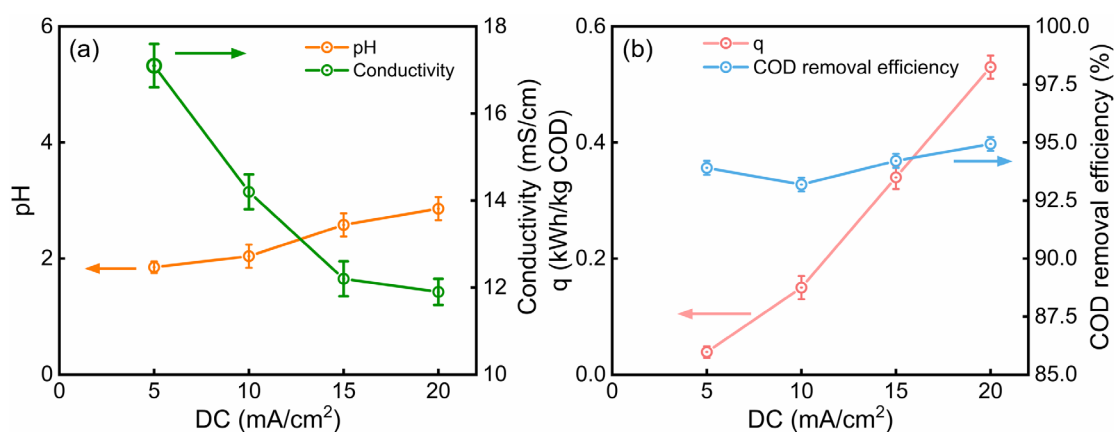
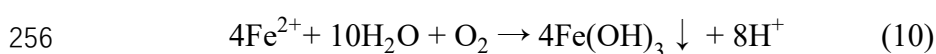
232 Current density was the main factor affecting the removal of pollutants during EC  
233 process. In Fig.2(a), when the applied current density increased from 5 to 20 mA/cm<sup>2</sup>,  
234 the pH of the effluent increased from 1.85 to 2.86, while the conductivity decreased  
235 from 17.9 to 11.9 mS/cm. These results were due to the constant consumption of  
236 hydrogen ions during the EC process. VERW in the reaction tank was disturbed by the  
237 hydrogen produced near the cathode (equation (8)). Moreover, the gas was beneficial  
238 to the coagulation process<sup>[50,55]</sup>. Notably, the removal efficiency of COD decreased first  
239 and then increased with the increase of current density, reaching 94.9% at the current  
240 density of 20 mA/cm<sup>2</sup> (Fig.2(b)). As shown in equations (8-10), this phenomenon was  
241 related to the removal of organic matters by air flotation and flocculation precipitation  
242 in EC process<sup>[36,56]</sup>. Previous study suggested that many small bubbles were conducive  
243 to the removal of pollutants during the flotation process and the bubble size increased  
244 with the increase of current density<sup>[57]</sup>. When the current density increased to 10  
245 mA/cm<sup>2</sup>, the COD removal efficiency decreased due to the increased of bubble volume.  
246 With the further increase of current density, the production of coagulants and bubbles  
247 increased, thereby increasing COD removal efficiency with the increase of current  
248 density. However, higher current density led to more energy being consumed, from an  
249 initial 0.039 to 0.53 kWh/kg COD at 20 mA/cm<sup>2</sup>. Consequently, the current density of

250 15 mA/cm<sup>2</sup> was selected as the optimum value for the COD removal efficiency with  
 251 low energy consumption.

252 At cathode:



254 At anode:



257

258 **Fig.2** Performance of EC with different current densities. (a) pH and conductivity of  
 259 the effluent, (b) COD removal efficiency and energy consumption. (PAM = 10 mg/L,  
 260 effluent volume = 50 mL).

261

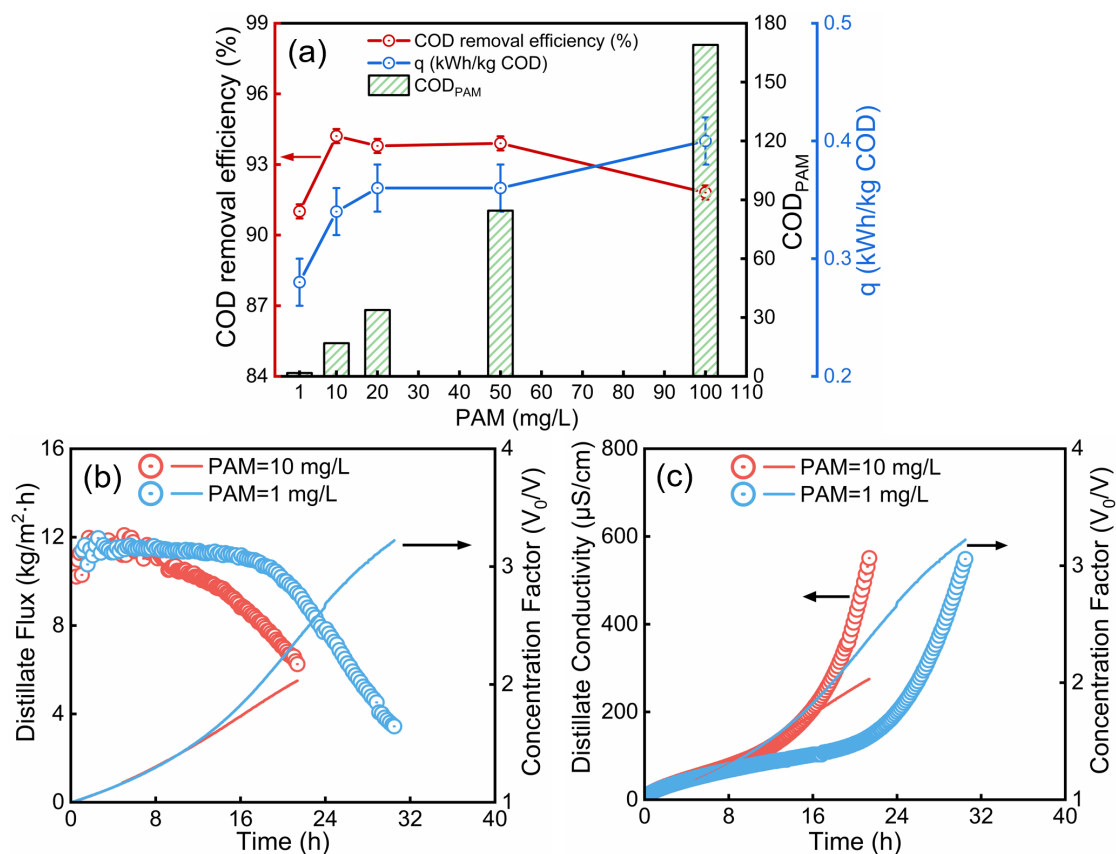
### 262 3.1.2 Effect of PAM dosage

263 A series of PAM experiments were carried out under the optimal current density  
 264 to define the optimal dosage of PAM. As shown in Fig.3(a), when the dosage of PAM  
 265 increased to 100 mg/L, the COD concentration in wastewater increased to 169.0 mg/L,  
 266 while the COD removal efficiency decreased from 94.2 to 91.8%. Moreover, the energy  
 267 consumption increased from 0.28 to 0.40 kWh/kg COD. These results indicated that the

268 overdosage of PAM led to a decrease in COD removal efficiency and an increase in  
269 energy consumption. On one hand, the addition of PAM increased the COD load,  
270 resulting in a decrease of COD removal efficiency. On the other hand, PAM overdosage  
271 destabilized and redissolved steady-state pollutants in VERW, increasing the  
272 concentration of COD<sup>[57]</sup>. When the dosage of PAM was 1 mg/L, the system energy  
273 consumption was low to 0.28 kWh/kg COD. When the dosage of PAM was 10 mg/L,  
274 the COD removal efficiency was the highest. Consequently, a lower dosage of PAM  
275 was beneficial to the EC process.

276 The impact of adding 10 mg/L PAM in the EC process on DCMD system  
277 performance was more significant than addition of 1 mg/L. In Fig.3(b-c), when the  
278 PAM dosage was 10 mg/L, the system flux decreased significantly after 8 hours, and  
279 the conductivity increased sharply after 12 hours, reaching 550  $\mu$ S/cm until 21 hours.  
280 In contrast, when the PAM dosage was 1 mg/L, the flux remained stable for a longer  
281 time, gradually decreased at 20 h, and reached the same conductivity at 30.5 h. At the  
282 end of the experiment, the CF of DCMD system with the PAM dosage of 1 mg/L was  
283 3.2, which was higher than that with the PAM dosage of 10 mg/L, indicating that the  
284 DCMD process after the EC pretreatment with addition of less flocculant could recover  
285 more distillate. This phenomenon can be attributed to the PVDF membrane fouling by  
286 PAM. The added PAM molecules might adhere to or deposit on the external surface of  
287 the membrane via establishing non-specific interactions with the functional groups of  
288 membrane materials, adding additional mass transfer resistance<sup>[58]</sup>. In addition, PAM  
289 molecules might trap inside the membrane pores, reducing the pore size and enhancing

290 the resistance to vapor transfer. Especially, PAM has high tendency to interact with each  
 291 other at high concentrations<sup>[59]</sup>. The result that adverse effects of adding large amounts  
 292 of PAM in feed on DCMD was also reported in previous studies<sup>[59]</sup>. In conclusion, 1  
 293 mg/L was selected as the optimal PAM dosage in the EC process.



294  
 295 **Fig. 3** Effect of PAM dosage on organic matter removal efficiency, COD contribution  
 296 and energy consumption in the continuous EC process (a); DCMD system performance,  
 297 CF with (b) distillate flux and (c) distillate conductivity as a function of time during  
 298 treatment of VERW ( $I = 1.5$  A, PAM dosage = 1 and 10 mg/L).

299

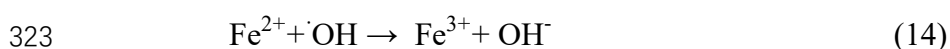
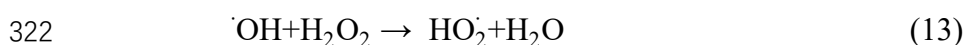
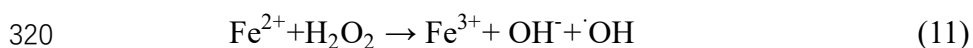
### 300 3.2 Organics removal via PEC

#### 301 3.2.1 Effect of H<sub>2</sub>O<sub>2</sub> dosage

302 Although the COD of the VERW was significantly reduced via the continuous

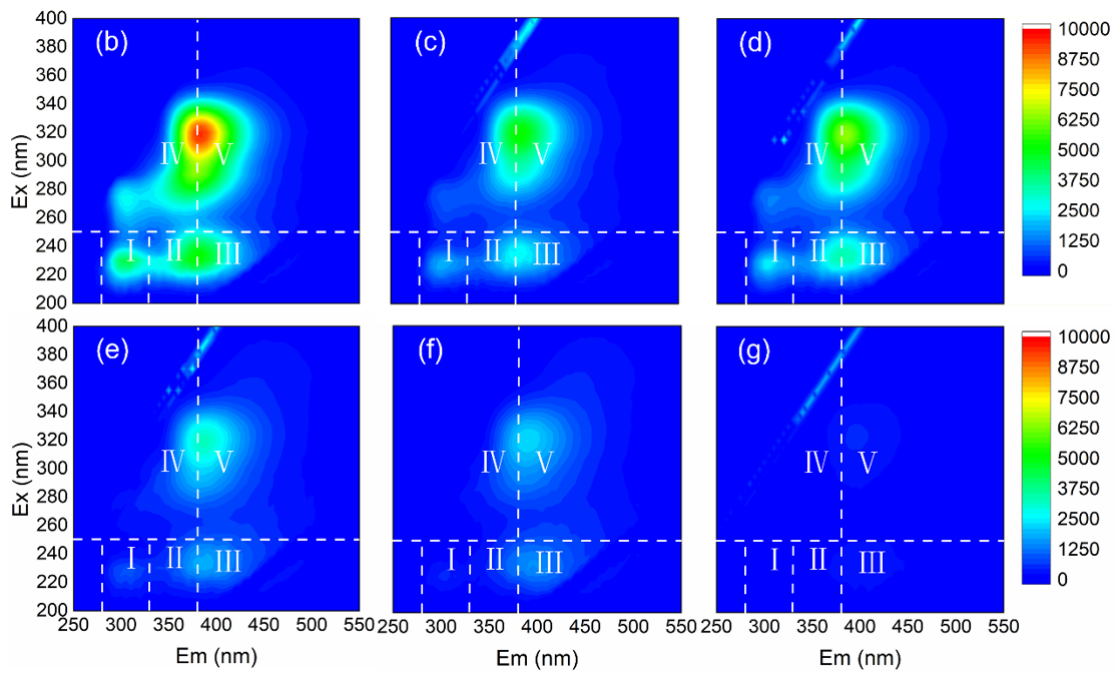
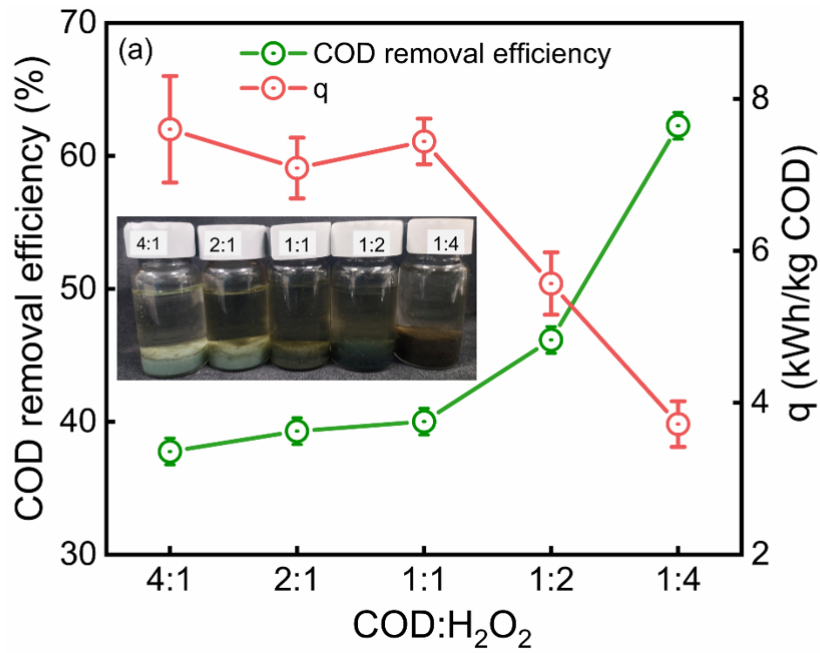


303 flow EC process, the effluent of VERW treated by EC still contains about 10% COD  
 304 with a concentration of 2136.6 mg/L. Herein the PEC was used to further treat the  
 305 effluent from EC process. As shown in Fig.4(a), the COD removal efficiency increased  
 306 with the increase of H<sub>2</sub>O<sub>2</sub> dosage. In addition, the energy consumption decreased with  
 307 the increase of the H<sub>2</sub>O<sub>2</sub> dosage, which was possibly due to the sharp increase of the  
 308 COD removal efficiency. Specifically, when the addition dosage of H<sub>2</sub>O<sub>2</sub> was equal to  
 309 a quarter of the COD concentration, the COD concentration of the effluent from PEC  
 310 was 1329.7 mg/L, and the energy consumption was 7.6 kWh/kg COD. When the dosage  
 311 of H<sub>2</sub>O<sub>2</sub> increased to four times of the COD concentration, the COD concentration  
 312 decreased to 806.4 mg/L, the removal efficiency increased to 62.3%, and the energy  
 313 consumption decreased to 3.72 kWh/kg COD. Interestingly, with the increase of H<sub>2</sub>O<sub>2</sub>  
 314 dosage, the color of precipitation gradually changed from light green to dark green, and  
 315 finally to reddish brown (shown in Fig.4(a)). The reason for the phenomenon occurred  
 316 was that more Fe<sup>2+</sup> ions were oxidized to Fe<sup>3+</sup> ions (equation 11). However, with the  
 317 increase of H<sub>2</sub>O<sub>2</sub> dosage, the Fenton reaction was inhibited (equation 12-14)<sup>[60, 61]</sup>.  
 318 Therefore, it was unsuitable to further increase the addition dosage of H<sub>2</sub>O<sub>2</sub>, and the  
 319 optimal H<sub>2</sub>O<sub>2</sub> dosage was four times of the COD concentration of the EC effluent.



324 To further characterize the organic pollutants removed via EC-PEC process, 3D-

325 EEM fluorescence spectra of the influent and effluent were illustrated in Fig.4(b-g).  
326 The fluorescence peaks of organics in the influent were mainly distributed in region V,  
327 IV, III, and I (Fig.4(b)). The peaks in region V and III were related to humic acid-like  
328 and fulvic acid-like substances, respectively. Peaks at 230.0/310.0 (Ex/Em(nm)) and  
329 280.0/310.0 (Ex/Em(nm)) in the region I and IV might represent BPA<sup>[62, 63]</sup>. The  
330 fluorescence peak intensity of the organic in effluent weakened gradually with the  
331 increase of the H<sub>2</sub>O<sub>2</sub> dosage. Result confirmed that the PEC was an effective process  
332 for organics removal. Notably, with the increase of H<sub>2</sub>O<sub>2</sub> addition dosage, the  
333 characteristic peaks of BPA (Fig.4(e)) disappeared before the peaks in region III and V  
334 (Fig.4(g)) disappeared. The result indicated that PEC process was particularly effective  
335 in removing BPA. Similar results were found in previous study by Escalona et al. where  
336 a small amount of H<sub>2</sub>O<sub>2</sub> could quickly remove most of BPA in wastewater<sup>[64]</sup>. There  
337 was no obvious fluorescence peak observed in Fig.4(g), which indicated that most of  
338 the fluorescent organics was removed.



339

340 **Fig.4** Effect of COD/H<sub>2</sub>O<sub>2</sub> mass ratios on PEC process, (a) energy consumption and

341 COD removal efficiency; 3D-EEM spectra of influent (b) and effluent, COD/H<sub>2</sub>O<sub>2</sub> mass

342 ratios were (c) 4:1, (d) 2:1, (e) 1:1, (f) 1:2 and (g) 1:4 respectively (25 times dilution).

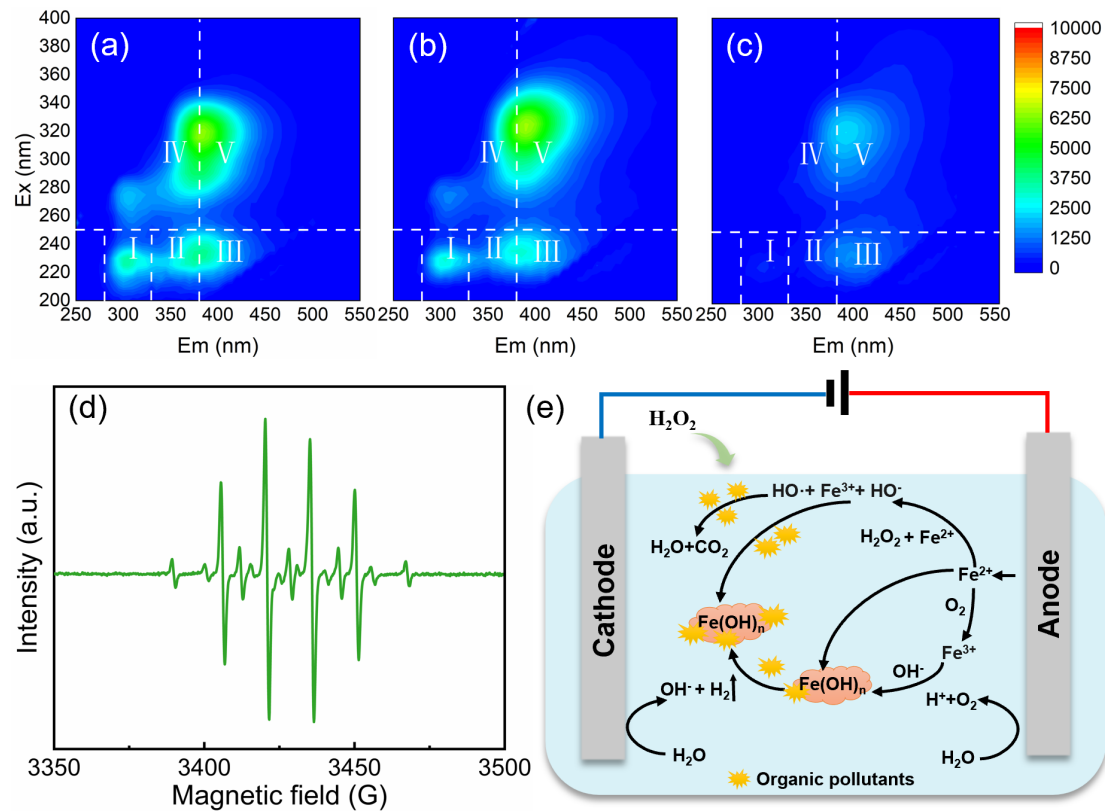
343

### 344 **3.2.2 Mechanism of organics removal via PEC**

345 The generation and occurrence of hydroxyl radicals during the PEC process was

346 determined by electron paramagnetic resonance (EPR) spectroscopy (Fig.5(d)).

347 Subsequently, the removal mechanism of organics via the PEC process was verified by  
348 the quenching experiments on the hydroxyl radicals. In this work, methanol was used  
349 as the quenching agent and the dosage was determined according to relevant reports<sup>[65,</sup>  
350 <sup>66]</sup>. Meanwhile, the effect of coagulation on organics removal via the PEC process was  
351 determined by comparing the EEM spectra results of quenching experiments (Fig.5(b)),  
352 double-EC experiment (Fig.5(a)) and EC experiment (Fig.4(b)). The weak intensity of  
353 the fluorescent peak reported in Fig.5(a) meant that some contaminants were removed  
354 by coagulation during the PEC process. Moreover, similar EEM spectra of the  
355 quenching experiment (Fig.5(b)) and double-EC experiment (Fig.5(a)) indicated that  
356 coagulation did not contribute significantly to the removal of organics. On the contrary,  
357 the significant inhibitory effect of the methanol on the removal of organic (Fig.5(b) and  
358 (c)) indicated that the contribution of  $\cdot\text{OH}$  oxidation was more significant than  
359 coagulation. Removal mechanism of PEC process was shown in Fig.5(e), the  
360 combination of advanced oxidation and coagulation led to the removal of organic.  
361 Particularly, the  $\cdot\text{OH}$  was produced by the reaction of the  $\text{Fe}^{2+}$  generated on the anode  
362 with  $\text{H}_2\text{O}_2$ . PEC process realized the reutilization of residual  $\text{Fe}^{2+}$  during the EC  
363 demulsification process and enhance the organic removal by advanced oxidation.  
364



365

366 **Fig.5** Organics removal in PEC process, 3D-EEM spectra of effluent treated with (a)  
 367 double EC experiment, (b) with quenching agent, (c) without quenching agent (25 times  
 368 dilution); (d) EPR spectra of hydroxyl radicals; (e) mechanism of organics removal.

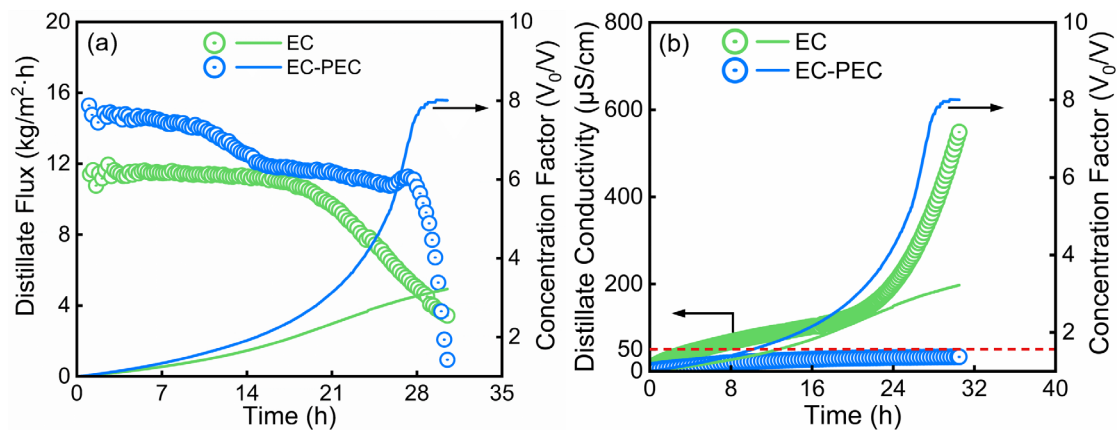
369

### 370 3.3 DCMD performance

#### 371 3.3.1 Effect of pretreatment on DCMD performance

372 The initial distillate flux of DCMD filtration of VERW pre-treated by EC was 11.4  
 373 kg/m<sup>2</sup>·h, while the flux of DCMD filtration of VERW pre-treated via EC-PEC increased  
 374 to 15.3 kg/m<sup>2</sup>·h (Fig.6(a)). The DCMD process maintained the stability of high  
 375 distillation flux for a long operating time. The conductivity of the distillate increased  
 376 sharply to 779 μS/cm at the end of DCMD filtration of VERW pre-treated by EC. The  
 377 corresponding CF was 3.4. In contrast, the DCMD filtration of VERW pre-treated via

378 EC-PEC kept running until the hot side water was insufficient for operation and the  
 379 conductivity remained below 33.3  $\mu\text{S}/\text{cm}$  (Fig.6(b)) with the CF finally reached up to  
 380 8.1. Results showed that after EC demulsification treatment, there were still pollutants  
 381 in the VERW that could result in membrane fouling. After further PEC treatment, the  
 382 degree of membrane fouling was mitigated due to the efficient removal of organics.  
 383 Therefore, the removal of organics via EC-PEC was considered as an effective  
 384 pretreatment process prior to DCMD filtration of VERW to reduce the volume of the  
 385 waste steam and recover a large amount of high-quality clean water.



386

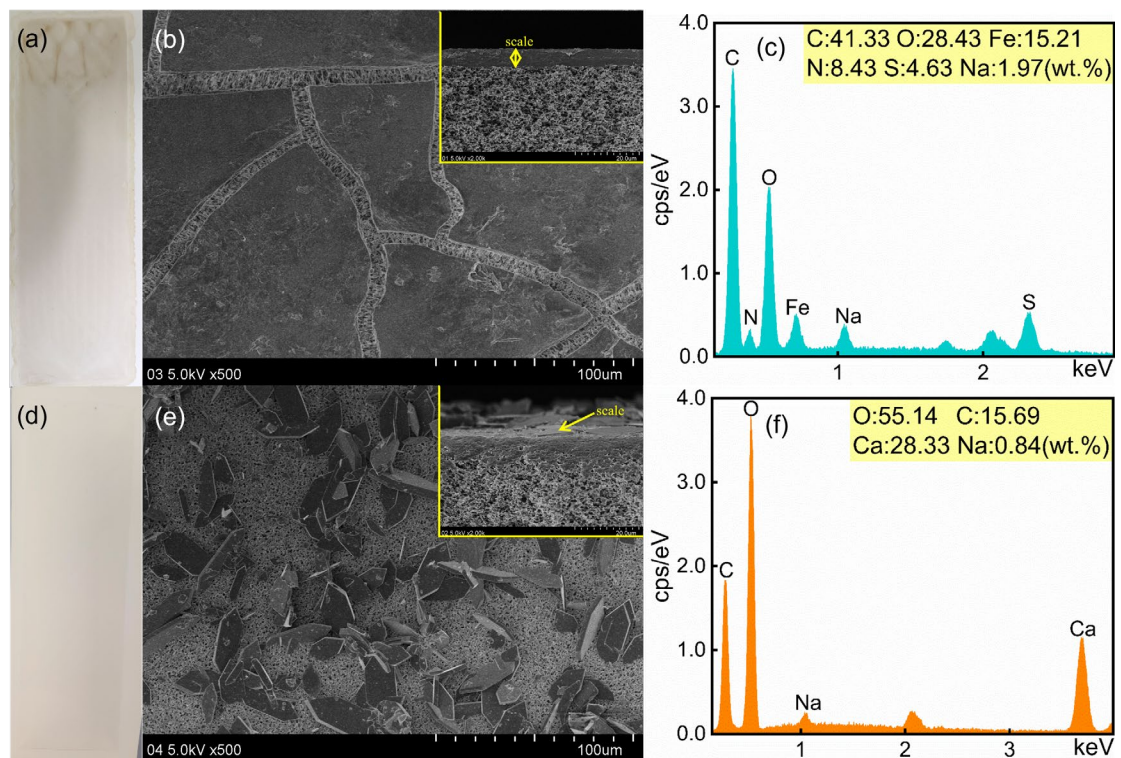
387 **Fig.6** Performance of DCMD filtration of VERW pre-treated by the continuous flow  
 388 EC and PEC process: CF with (a) distillate flux and (b) distillate conductivity as a  
 389 function of time during treatment of VERW ( $I=1.5$  A, PAM dosage =1 mg/L, COD:  
 390  $\text{H}_2\text{O}_2 = 1:4$ ).

391

### 392 3.3.2 Membrane autopsy

393 SEM-EDS was used to characterize the PVDF membrane to analyze the influence  
 394 of different pretreatment on membrane fouling. After DCMD filtration of VERW pre-  
 395 treated via EC, it was found that the brown deposits distributed on the membrane

396 surface (Fig.7(a)). Compared to the clean MD membranes (Fig.S5), there was a thick  
 397 fouling layer on the membrane surface composed of C, O, N, Fe, Na, and S (Fig.7(b-  
 398 c)). Based on the results, it can be reasonably speculated that the foulants were mixture  
 399 of organics and salt containing sodium and iron. On the contrary, the membrane  
 400 obtained from DCMD filtration of VERW pre-treated via EC-PEC was almost clean  
 401 without obvious fouling layer (Fig.7(d)). According to SEM-EDS analysis, only a small  
 402 amount of calcium carbonate crystals was randomly deposited on the membrane surface  
 403 (Fig.7(e-f)). As the removal of dissolved organics in VERW via EC-PEC, membrane  
 404 fouling was significantly mitigated. Thus, organics in VERW were the main reason for  
 405 the deterioration of DCMD performance and acceleration of membrane fouling.



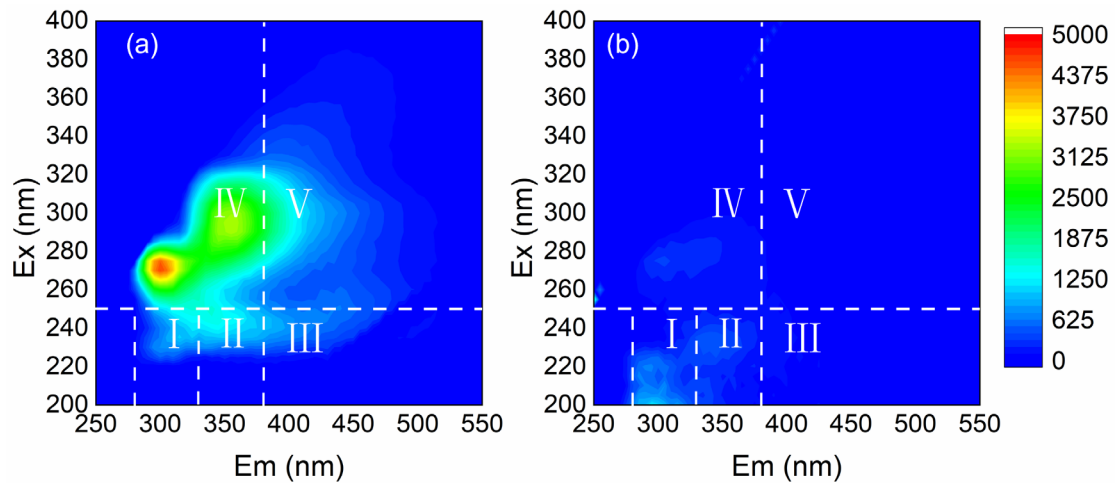
406  
 407 **Fig.7** The photos and SEM images of the surface and cross-section of the membranes  
 408 after DCMD filtration of VERW pre-treated via EC (a & b) and PEC (d & e), (c), and  
 409 the corresponding results of EDS analysis (f).

410

### 411 **3.3.2 Comparison of distillate quality**

412 The pH of the distillate after DCMD filtration of the VERW pre-treated by EC was  
413 3, with many metal ions and high COD, which indicated that the pollutants in the  
414 VERW were not rejected effectively via the DCMD process (Table S4). Moreover, the  
415 dissolved ions from the EC process partially permeates into the distillate during the  
416 DCMD filtration of VERW pre-treated via EC process. However, at the conclusion of  
417 DCMD filtration of VERW pre-treated via EC-PEC, the distillate was alkaline (pH =  
418 9), and only ammonia nitrogen was detected. Volatilization and ionization of ammonia  
419 were the main reasons for the changes of the pH and conductivity of the distillate. In  
420 addition, the lower COD concentration of the distillate may be due to the  
421 transmembrane transport of volatile organic compounds. EEM spectra showed that the  
422 organics in the distillate after DCMD filtration of VERW pre-treated via EC-PEC were  
423 distributed in region IV, and the two strong fluorescence peaks at 270.0/300.0 (Ex/Em  
424 (nm)) and 290.0/355.0 (Ex/Em (nm)) represented BPA<sup>[62]</sup>. The distillate of the DCMD  
425 filtration of the VERW pre-treated by EC-PEC detected no obvious fluorescence peak  
426 (Fig.8). In summary, the DCMD process as an advanced treatment approach provided  
427 a potential alternative for treatment of the waste steam pre-treated by EC-PEC from  
428 resin production.





429

430 **Fig.8** 3D-EEM spectra of organic pollutants in distillate after (a) EC pretreatment (b)

431 PEC pretreatment.

432

#### 433 **4. Conclusion**

434 In this work, the continuous flow EC and PEC processes were used as the  
 435 pretreatment approaches prior to advanced treatment of VERW via DCMD. The  
 436 optimization of the two pretreatment processes was conducted. Besides, system  
 437 performance and membrane fouling of DCMD filtration of the VERW pre-treated by  
 438 the two different pretreatment processes were evaluated. The main conclusions were  
 439 summarized as follows:

- 440 • Continuous flow EC and PEC processes were effective to remove the organics in  
 441 VERW. The optimal current density and PAM dosage was 15 mA/cm<sup>2</sup> and 1 mg/L,  
 442 respectively in EC process. For the PEC process, the optimal H<sub>2</sub>O<sub>2</sub> dosage was four  
 443 times of EC effluent COD concentration.
- 444 • The energy consumption of the continuous flow EC and PEC process under the  
 445 optimal conditions was 0.34 kWh/kg COD and 3.72 kWh/kg COD, respectively.

- 446 • The initial flux of DCMD filtration of VERW pre-treated via EC-PEC increased by  
447 35%, and membrane fouling was significantly mitigated, compared with that pre-  
448 treated by EC.
- 449 • The volume of VERW was reduced via DCMD with evidence that the CF reached  
450 up to 8.1. Additionally, the high-quality distillate with conductivity less than 33.2  
451  $\mu\text{S}/\text{cm}$  was obtained.

452

### 453 **Acknowledgements**

454 The authors would like to thank the financial support from Natural Science  
455 Foundation of Shanghai (No.20ZR1400100).

## 456 References

- 457 [1] S. Yang, H. Fang, H. Li, F. Shen, X. Chen, Y. Hu, Z. Yang, Synthesis of tung oil-based  
458 vinyl ester resin and its application for anti-corrosion coatings, *Prog. Org. Coat.* 170 (2022). <https://doi.org/10.1016/j.porgcoat.2022.106967>.  
459
- 460 [2] S. Jaswal, B. Gaur, New trends in vinyl ester resins, *Rev. Chem. Eng.* 30(6) (2014). <https://doi.org/10.1515/revce-2014-0012>.  
461
- 462 [3] C. Jang, T.E. Lacy, S.R. Gwaltney, H. Toghiani, C.U. Pittman, Relative Reactivity Volume  
463 Criterion for Cross-Linking: Application to Vinyl Ester Resin Molecular Dynamics Simulations,  
464 *Macromolecules* 45(11) (2012) 4876-4885. <https://doi.org/10.1021/ma202754d>.  
465
- 466 [4] F.-Q. Zhang, Y.-Z. Zhao, Y.-J. Xu, Y. Liu, P. Zhu, Flame retardation of vinyl ester resins  
467 and their glass fiber reinforced composites via liquid DOPO-containing 1-vinylimidazole salts,  
468 *Compos. Part B Eng.* 234 (2022). <https://doi.org/10.1016/j.compositesb.2022.109697>.  
469
- 470 [5] B.K. Kandola, J.R. Ebdon, C. Zhou, Development of vinyl ester resins with improved flame  
471 retardant properties for structural marine applications, *React. Funct. Polym.* 129 (2018) 111-1  
472 22. <https://doi.org/10.1016/j.reactfunctpolym.2017.08.006>.  
473
- 474 [6] S. Dev, P.N. Shah, Y. Zhang, D. Ryan, C.J. Hansen, Y. Lee, Synthesis and mechanical pro  
475 perties of flame retardant vinyl ester resin for structural composites, *Polymer* 133 (2017) 20-29.  
476 <https://doi.org/10.1016/j.polymer.2017.11.017>.  
477
- 478 [7] H. Gai, X. Zhang, S. Chen, C. Wang, M. Xiao, T. Huang, J. Wang, H. Song, An improve  
479 d tar-water separation process of low-rank coal conversion wastewater for increasing the tar yi  
480 eld and reducing the oil content in wastewater, *Chem. Eng. J.* 383 (2020) 123229. <https://doi.org/10.1016/j.ccej.2019.123229>.  
481
- 482 [8] M. Ahmadi, H. Amiri, S.S. Martínez, Treatment of phenol-formaldehyde resin manufacturin  
483 g wastewater by the electrocoagulation process, *Desalination and Water Treatment* 39(1-3) (201  
484 2) 176-181. <https://doi.org/10.1080/19443994.2012.669172>.  
485
- 486 [9] L. Jiang, L. Chen, L. Zhu, In-situ electric-enhanced membrane distillation for simultaneous  
487 flux-increasing and anti-wetting, *J. Membr. Sci.* 630 (2021) 119305. <https://doi.org/10.1016/j.memsci.2021.119305>.  
488
- 489 [10] W. Zhong, L. Guo, C. Ji, G. Dong, S. Li, Membrane distillation for zero liquid discharge  
490 during treatment of wastewater from the industry of traditional Chinese medicine: a review, *E  
491 nviron. Chem. Lett.* 19(3) (2021) 2317-2330. <https://doi.org/10.1007/s10311-020-01162-y>.  
492
- 493 [11] C. Liu, L. Zhu, R. Ji, H. Xiong, Zero liquid discharge treatment of brackish water by me  
494 mbrane distillation system: Influencing mechanism of antiscalants on scaling mitigation and biof  
495 ilm formation, *Sep. Purif. Technol.* 282 (2022) 120157. [https://doi.org/10.1016/j.seppur.2021.1201  
496 57](https://doi.org/10.1016/j.seppur.2021.120157).  
497
- 498 [12] M.M.A. Shirazi, L.F. Dumée, Membrane distillation for sustainable wastewater treatment, *J.  
499 Water Process. Eng.* 47 (2022) 102670. <https://doi.org/10.1016/j.jwpe.2022.102670>.  
500
- 501 [13] L. Camacho, L. Dumée, J. Zhang, J.-d. Li, M. Duke, J. Gomez, S. Gray, Advances in M  
502 embrane Distillation for Water Desalination and Purification Applications, *Water* 5(1) (2013) 94  
503 -196. <https://doi.org/10.3390/w5010094>.  
504
- 505 [14] K. Sardari, P. Fyfe, D. Lincicome, S. Ranil Wickramasinghe, Combined electrocoagulation  
506 and membrane distillation for treating high salinity produced waters, *J. Membr. Sci.* 564 (2018)  
507 82-96. <https://doi.org/10.1016/j.memsci.2018.06.041>.  
508

499 [15] O.R. Lokare, S. Tavakkoli, G. Rodriguez, V. Khanna, R.D. Vidic, Integrating membrane di  
500 stillation with waste heat from natural gas compressor stations for produced water treatment in  
501 Pennsylvania, *Desalination* 413 (2017) 144-153. <https://doi.org/10.1016/j.desal.2017.03.022>.

502 [16] R. Sallakhniknezhad, A.S. Niknejad, M. Barani, E. Ranjbari, S. Bazgir, A. Kargari, M. Ra  
503 souli, S. Chae, Hypersaline drilling mud water treatment using pretreatment-free DCMD proces  
504 s, *Desalination* 539 (2022) 115938. <https://doi.org/10.1016/j.desal.2022.115938>.

505 [17] Z. Yan, H. Yang, F. Qu, H. Yu, H. Liang, G. Li, J. Ma, Reverse osmosis brine treatment  
506 using direct contact membrane distillation: effects of feed temperature and velocity, *Desalinatio  
507 n* 423 (2017) 149-156. <https://doi.org/10.1016/j.desal.2017.09.010>.

508 [18] M.T.T. Ngo, B.Q. Diep, H. Sano, Y. Nishimura, S. Boivin, H. Kodamatani, H. Takeuchi,  
509 S.C.W. Sakti, T. Fujioka, Membrane distillation for achieving high water recovery for potable  
510 water reuse, *Chemosphere* 288 (2022) 132610. <https://doi.org/10.1016/j.chemosphere.2021.132610>.

511 [19] Z. Anari, A. Sengupta, K. Sardari, S.R. Wickramasinghe, Surface modification of PVDF  
512 membranes for treating produced waters by direct contact membrane distillation, *Sep. Purif. Tec  
513 hnol.* 224 (2019) 388-396. <https://doi.org/10.1016/j.seppur.2019.05.032>.

514 [20] M. Yao, Y.C. Woo, L.D. Tijing, J.-S. Choi, H.K. Shon, Effects of volatile organic compo  
515 unds on water recovery from produced water via vacuum membrane distillation, *Desalination* 4  
516 40 (2018) 146-155. <https://doi.org/10.1016/j.desal.2017.11.012>.

517 [21] Y. Hu, M. Xie, G. Chen, M. Huang, W. Tan, Nitrogen recovery from a palladium leachat  
518 e via membrane distillation: System performance and ammonium chloride crystallization, *Resou  
519 r. Conserv. Recycl.* 183 (2022). <https://doi.org/10.1016/j.resconrec.2022.106368>.

520 [22] J. Ren, J. Li, Z. Chen, F. Cheng, Fate and wetting potential of bio-refractory organics in  
521 membrane distillation for coke wastewater treatment, *Chemosphere* 208 (2018) 450-459. [https://  
522 doi.org/10.1016/j.chemosphere.2018.06.002](https://doi.org/10.1016/j.chemosphere.2018.06.002).

523 [23] S. Cao, W. Jiang, M. Zhao, A. Liu, M. Wang, Q. Wu, Y. Sun, Pretreatment Hydrolysis  
524 Acidification/Two-Stage AO Combination Process to Treat High-Concentration Resin Production  
525 Wastewater, *Water* 14(19) (2022). <https://doi.org/10.3390/w14192949>.

526 [24] R. Ding, D. Zhang, Y. Gao, X. Chen, M. Yang, Characteristics of refractory organics in i  
527 ndustrial wastewater treated using a Fenton-coagulation process, *Environ. Technol.* 42(22) (2021)  
528 3432-3440. <https://doi.org/10.1080/09593330.2020.1732476>.

529 [25] M. Manna, S. Sen, Advanced oxidation process: a sustainable technology for treating refra  
530 ctory organic compounds present in industrial wastewater, *Environ. Sci. Pollut. Res. Int.* (202  
531 2). <https://doi.org/10.1007/s11356-022-19435-0>.

532 [26] S. Li, Y. Yang, H. Zheng, Y. Zheng, T. Jing, J. Ma, J. Nan, Y.K. Leong, J.S. Chang, Ad  
533 vanced oxidation process based on hydroxyl and sulfate radicals to degrade refractory organic  
534 pollutants in landfill leachate, *Chemosphere* 297 (2022) 134214. [https://doi.org/10.1016/j.chemos  
535 phere.2022.134214](https://doi.org/10.1016/j.chemosphere.2022.134214).

536 [27] M.B. Asif, Z. Fida, A. Tufail, J.P. van de Merwe, F.D.L. Leusch, B.K. Pramanik, W.E. P  
537 rice, F.I. Hai, Persulfate oxidation-assisted membrane distillation process for micropollutant degr  
538 adation and membrane fouling control, *Sep. Purif. Technol.* 222 (2019) 321-331. [https://doi.org/  
539 10.1016/j.seppur.2019.04.035](https://doi.org/10.1016/j.seppur.2019.04.035).

540 [28] B. Ji, M. Bilal Asif, Z. Zhang, Photothermally-activated peroxydisulfate (PMS) pretreat  
541 ment for fouling alleviation of membrane distillation of surface water: Performance and mechan  
542 ism, *Sep. Purif. Technol.* 309 (2023). <https://doi.org/10.1016/j.seppur.2022.123043>.

543 [29] X. Zhao, X. Wei, P. Xia, H. Liu, J. Qu, Removal and transformation characterization of r  
544 efractory components from biologically treated landfill leachate by Fe<sup>2+</sup>/NaClO and Fenton oxi  
545 dation, *Sep. Purif. Technol.* 116 (2013) 107-113. <https://doi.org/10.1016/j.seppur.2013.05.030>.

546 [30] K. Swain, B. Abbassi, C. Kinsley, Combined Electrocoagulation and Chemical Coagulation  
547 in Treating Brewery Wastewater, *Water* 12(3) (2020). <https://doi.org/10.3390/w12030726>.

548 [31] Y.X. Zhao, B.Y. Gao, G.Z. Zhang, Q.B. Qi, Y. Wang, S. Phuntsho, J.H. Kim, H.K. Shon,  
549 Q.Y. Yue, Q. Li, Coagulation and sludge recovery using titanium tetrachloride as coagulant fo  
550 r real water treatment: A comparison against traditional aluminum and iron salts, *Sep. Purif. Te  
551 chnol.* 130 (2014) 19-27. <https://doi.org/10.1016/j.seppur.2014.04.015>.

552 [32] J. Ding, M. Jiang, G. Zhao, L. Wei, S. Wang, Q. Zhao, Treatment of leachate concentrate  
553 by electrocoagulation coupled with electro-Fenton-like process: Efficacy and mechanism, *Sep.  
554 Purif. Technol.* 255 (2021). <https://doi.org/10.1016/j.seppur.2020.117668>.

555 [33] F.F. Nyouna, S.R. Tchamango, N. Benjamin Espoir, R. Domga, M.B. Ngassoum, A Study  
556 of Electrocoagulation for Treatment of Wastewater from Oil Change Applying of Iron Electrode  
557 s, *International Journal of ChemTech Research* 12(03) (2019) 169-176. [https://doi.org/10.20902/ij  
558 ctr.2019.120324](https://doi.org/10.20902/ijctr.2019.120324).

559 [34] A. Othmani, A. Kadier, R. Singh, C.A. Igwegbe, M. Bouzid, M.O. Aquatar, W.A. Khanda  
560 y, M.E. Bote, F. Damiri, O. Gokkus, F. Sher, A comprehensive review on green perspectives o  
561 f electrocoagulation integrated with advanced processes for effective pollutants removal from w  
562 ater environment, *Environ. Res.* 215(Pt 1) (2022) 114294. [https://doi.org/10.1016/j.envres.2022.11  
563 4294](https://doi.org/10.1016/j.envres.2022.114294).

564 [35] F. Sher, K. Hanif, S.Z. Iqbal, M. Imran, Implications of advanced wastewater treatment: E  
565 lectrocoagulation and electroflocculation of effluent discharged from a wastewater treatment plan  
566 t, *J. Water Process. Eng.* 33 (2020) 101101. <https://doi.org/10.1016/j.jwpe.2019.101101>.

567 [36] K. Eryuruk, U. Tezcan Un, U. Bakır Oğutveren, Electrochemical treatment of wastewaters  
568 from poultry slaughtering and processing by using iron electrodes, *J. Clean. Prod.* 172 (2018)  
569 1089-1095. <https://doi.org/10.1016/j.jclepro.2017.10.254>.

570 [37] S.R.S. Bandaru, C.M. van Genuchten, A. Kumar, S. Glade, D. Hernandez, M. Nahata, A.  
571 Gadgil, Rapid and Efficient Arsenic Removal by Iron Electrocoagulation Enabled with in Situ  
572 Generation of Hydrogen Peroxide, *Environ. Sci. Technol.* 54(10) (2020) 6094-6103. [https://doi.o  
573 rg/10.1021/acs.est.0c00012](https://doi.org/10.1021/acs.est.0c00012).

574 [38] T. Mori, H. Nagashima, Y. Ito, Y. Era, J. Tsubaki, Agglomeration of fine particles in wat  
575 er upon application of DC electric field, *Miner. Eng.* 133 (2019) 119-126. [https://doi.org/10.101  
576 6/j.mineng.2019.01.017](https://doi.org/10.1016/j.mineng.2019.01.017).

577 [39] A. Ikhlq, F. Javed, A. Akram, A. Rehman, F. Qi, M. Javed, M.J. Mehdi, F. Waheed, S.  
578 Naveed, H.A. Aziz, Synergic catalytic ozonation and electroflocculation process for the treatme  
579 nt of veterinary pharmaceutical wastewater in a hybrid reactor, *J. Water Process. Eng.* 38 (202  
580 0). <https://doi.org/10.1016/j.jwpe.2020.101597>.

581 [40] Z. Al-Qodah, Y. Al-Qudah, E. Assirey, Combined biological wastewater treatment with ele  
582 ctrocoagulation as a post-polishing process: A review, *Sep. Sci. Technol.* 55(13) (2019) 2334-23  
583 52. <https://doi.org/10.1080/01496395.2019.1626891>.

584 [41] Z. Al-Qodah, Y. Al-Qudah, W. Omar, On the performance of electrocoagulation-assisted bi  
585 ological treatment processes: a review on the state of the art, *Environ. Sci. Pollut. Res. Int.* 26  
586 (28) (2019) 28689-28713. <https://doi.org/10.1007/s11356-019-06053-6>.

587 [42] Z. Al-Qodah, M. Al-Shannag, K. Bani-Melhem, E. Assirey, M.A. Yahya, A. Al-Shawabkeh,  
588 h, Free radical-assisted electrocoagulation processes for wastewater treatment, *Environ. Chem. Lett.*  
589 *16*(3) (2018) 695-714. <https://doi.org/10.1007/s10311-018-0711-1>.

590 [43] X. Jin, X. Xie, S. Zhang, C. Yang, L. Xu, X. Shi, P. Jin, X.C. Wang, Insights into the electro-hybrid  
591 ozonation-coagulation process—Significance of connection configurations and electrode types, *Water Res.*  
592 *204* (2021) 117600. <https://doi.org/10.1016/j.watres.2021.117600>.

593 [44] E. Yüksel, İ.A. Şengil, M. Özacar, The removal of sodium dodecyl sulfate in synthetic wastewater by  
594 peroxi-electrocoagulation method, *Chem. Eng. J.* *152*(2-3) (2009) 347-353. <https://doi.org/10.1016/j.cej.2009.04.058>.

595  
596 [45] Z. Qiang, J.-H. Chang, C.-P. Huang, Electrochemical regeneration of Fe<sup>2+</sup> in Fenton oxidation  
597 processes, *Water Res.* *37*(6) (2003) 1308-1319. [https://doi.org/10.1016/s0043-1354\(02\)00461-x](https://doi.org/10.1016/s0043-1354(02)00461-x).

598  
599 [46] W. Liang, G. Chen, M. Huang, Performance and membrane fouling mitigation for bio-treated  
600 coking wastewater treatment via membrane distillation: Effect of pre-treatment, *J. Water Process. Eng.*  
601 *46* (2022). <https://doi.org/10.1016/j.jwpe.2022.102647>.

602 [47] L. Chen, F. Li, F. He, Y. Mao, Z. Chen, Y. Wang, Z. Cai, Membrane distillation combined  
603 with electrocoagulation and electrooxidation for the treatment of landfill leachate concentrate, *Sep. Purif. Technol.*  
604 *291* (2022). <https://doi.org/10.1016/j.seppur.2022.120936>.

605 [48] M. Jebur, Y.-H. Chiao, K. Thomas, T. Patra, Y. Cao, K. Lee, N. Gleason, X. Qian, Y. Hu, M. Malmali,  
606 S.R. Wickramasinghe, Combined electrocoagulation-microfiltration-membrane distillation for  
607 treatment of hydraulic fracturing produced water, *Desalination* *500* (2021). <https://doi.org/10.1016/j.desal.2020.114886>.

608  
609 [49] Y. Hu, Y. Xu, M. Xie, M. Huang, G. Chen, Characterization of scalants and strategies for  
610 scaling mitigation in membrane distillation of alkaline concentrated circulating cooling water, *Desalination*  
611 *527* (2022). <https://doi.org/10.1016/j.desal.2021.115534>.

612 [50] E. Butler, Y.-T. Hung, R.Y.-L. Yeh, M. Suleiman Al Ahmad, Electrocoagulation in Wastewater  
613 Treatment, *Water* *3*(2) (2011) 495-525. <https://doi.org/10.3390/w3020495>.

614 [51] J. Li, J. Wu, H. Sun, F. Cheng, Y. Liu, Advanced treatment of biologically treated coking  
615 wastewater by membrane distillation coupled with pre-coagulation, *Desalination* *380* (2016) 43-  
616 51. <https://doi.org/10.1016/j.desal.2015.11.020>.

617 [52] J. Ding, M. Jiang, G. Zhao, L. Wei, S. Wang, Q. Zhao, Treatment of leachate concentrate  
618 by electrocoagulation coupled with electro-Fenton-like process: Efficacy and mechanism, *Sep. Purif. Technol.*  
619 *255* (2021) 117668. <https://doi.org/10.1016/j.seppur.2020.117668>.

620 [53] C.A. Stedmon, R. Bro, Characterizing dissolved organic matter fluorescence with parallel factor  
621 analysis: a tutorial, *Limnol. Oceanogr. Methods* *6*(11) (2008) 572-579. <https://doi.org/10.4319/lom.2008.6.572>.

622  
623 [54] Y.K. Lee, S. Hong, J. Hur, A fluorescence indicator for source discrimination between microplastic-derived  
624 dissolved organic matter and aquatic natural organic matter, *Water Res.* *207* (2021) 117833.  
625 <https://doi.org/10.1016/j.watres.2021.117833>.

626 [55] J.-Q. Jiang, N. Graham, C. André, G.H. Kelsall, N. Brandon, Laboratory study of electrocoagulation–  
627 flotation for water treatment, *Water Res.* *36*(16) (2002) 4064-4078. [https://doi.org/10.1016/S0043-1354\(02\)00118-5](https://doi.org/10.1016/S0043-1354(02)00118-5).

628  
629 [56] M.K. Oden, H. Sari-Erkan, Treatment of metal plating wastewater using iron electrode by  
630 electrocoagulation process: Optimization and process performance, *Process Saf. Environ. Prot.* *1*

631 19 (2018) 207-217. <https://doi.org/10.1016/j.psep.2018.08.001>.

632 [57] X. Zhang, X. Zhang, Y. Liu, Q. Zhang, S. Yang, X. He, Removal of viscous and cloggin  
633 g suspended solids in the wastewater from acrylonitrile-butadiene-styrene resin production by a  
634 new dissolved air release device, *Process Saf. Environ. Prot.* 148 (2021) 524-535. <https://doi.org/10.1016/j.psep.2020.10.031>.

635 [58] S. Srisurichan, R. Jiratananon, A. Fane, Mass transfer mechanisms and transport resistan  
636 ces in direct contact membrane distillation process, *J. Membr. Sci.* 277(1-2) (2006) 186-194. <https://doi.org/10.1016/j.memsci.2005.10.028>.

637 [59] B. Hu, J. Ouyang, L. Jiang, Influence of flocculant polyacrylamide on concentration of tit  
638 anium white waste acid by direct contact membrane distillation, *Chin. J. Chem. Eng.* 28(9) (20  
639 20) 2483-2496. <https://doi.org/10.1016/j.cjche.2020.03.022>.

640 [60] V.K. Sandhwar, B. Prasad, Comparison of electrocoagulation, peroxi-electrocoagulation and  
641 peroxi-coagulation processes for treatment of simulated purified terephthalic acid wastewater: O  
642 ptimization, sludge and kinetic analysis, *Korean J. Chem. Eng.* 35(4) (2018) 909-921. <https://doi.org/10.1007/s11814-017-0336-2>.

643 [61] A.R. Yazdanbakhsh, M.R. Massoudinegad, S. Eliasi, A.S. Mohammadi, The influence of o  
644 perational parameters on reduce of azithromycin COD from wastewater using the peroxi -electro  
645 coagulation process, *J. Water Process. Eng.* 6 (2015) 51-57. <https://doi.org/10.1016/j.jwpe.2015.03.005>.

646 [62] W. Chen, P. Westerhoff, J.A. Leenheer, K. Booksh, Fluorescence Excitation–Emission Matr  
647 ix Regional Integration to Quantify Spectra for Dissolved Organic Matter, *Environ. Sci. Techno  
648 l.* 37(24) (2003) 5701-5710. <https://doi.org/10.1021/es034354c>.

649 [63] L. Chen, T. Maqbool, C. Hou, W. Fu, X. Zhang, Mechanistic study of oxidative removal  
650 of bisphenol A by pristine nanocatalyst Mn<sub>3</sub>O<sub>4</sub>/peroxymonosulfate, *Sep. Purif. Technol.* 281 (2  
651 022) 119882. <https://doi.org/10.1016/j.seppur.2021.119882>.

652 [64] I. Escalona, A. Fortuny, F. Stüber, C. Bengoa, A. Fabregat, J. Font, Fenton coupled with  
653 nanofiltration for elimination of Bisphenol A, *Desalination* 345 (2014) 77-84. <https://doi.org/10.1016/j.desal.2014.04.024>.

654 [65] L. Wang, B. Li, D.D. Dionysiou, B. Chen, J. Yang, J. Li, Overlooked Formation of H<sub>2</sub>O  
655 2 during the Hydroxyl Radical-Scavenging Process When Using Alcohols as Scavengers, *Enviro  
656 n. Sci. Technol.* 56(6) (2022) 3386-3396. <https://doi.org/10.1021/acs.est.1c03796>.

657 [66] R. Zhou, F. Liu, X. Du, C. Zhang, C. Yang, N.-A. Offiong, Y. Bi, W. Zeng, H. Ren, Re  
658 moval of metronidazole from wastewater by electrocoagulation with chloride ions electrolyte: T  
659 he role of reactive chlorine species and process optimization, *Sep. Purif. Technol.* 290 (2022) 1  
660 20799. <https://doi.org/10.1016/j.seppur.2022.120799>.

666